Active Fault-Tolerant LPV Control for Elevator Failure of Civil Aircraft Autolanding Based on Two-Stage Kalman Filter

Xudong Wang[a *], Shiqian Liu[b], Yuanjun Sang[c], and Guangrui Zhou[d]

School of Aeronautics and Astronautics, Shanghai Jiaotong University, Shanghai 200240, China

[a]hiwang@sjtu.edu.cn, [b]liushiqian@sjtu.edu.cn, [c]sangyuanjun@sjtu.edu.cn, [d]zgr2013@sjtu.edu.cn

Keywords: Aircraft landing; Linear parameter varying; Two-stage Kalman filter; Fault tolerant control.

Abstract: This paper presents an active fault-tolerant linear parameter varying (LPV) autolanding controller for a civil aircraft subject to elevator failure during landing maneuver. Firstly, an LPV autolanding controller is designed to assure the acceptable tracking performance and stability of the civil aircraft's autoland. The scheduling parameter is chosen as the estimation of the elevator failure factor. Secondly, a two-stage Kalman filter estimator is designed to estimate the failure factor. Then, the LPV controller and the estimator are integrated to achieve the active fault-tolerant performance. Finally, simulations of the autolanding control system show that a superior fault-tolerance can be achieved.

1. Introduction

For the civil aircraft, the automatic landing control system plays an important role to assist the pilot in the landing phase. However, the performance of the system will deteriorate when the aircraft is subjected to failures of actuators. Hence, a fault tolerant control (FTC) autolanding system that can sustain the effect of failures is important to aircraft's stability and reliability.

The neural network has been applied to design the FTC autolanding system [1,2]. However, the neural network method is only valid within the specific training set. A time delay control scheme was proposed for actuator failures during aircraft autolanding by Lee et al [3]. The LPV controller is adaptive to the scheduling parameters, which is a significant advantage over the fixed-gain controllers [4]. Liu et al [5] introduced an active FTC scheme for helicopter based on an LPV finite-time adaptive fault estimation method.

This paper designs an active FTC autolanding system for civil aircraft based on LPV control method. The elevator failure is regarded as the scheduling parameter and estimated by a two-stage Kalman filter. Section 2 deals with the linear model of civil aircraft, the LPV model with elevator failure and the landing maneuver. Section 3 describes the design of the FTC autolanding system. Section 4 presents some simulations to illustrate the performances of the designed LPV controller.

2. Dynamics Modelling and Problem Formulation

2.1 Longitudinal Linear Model of Civil Aircraft

The dynamic model of a civil aircraft can be built via Newton law, which is usually a standard six degrees of freedom equations of motion. And the nonlinear model of the aircraft can be trimmed and linearized via small disturbance linearized theory. For the purpose of autolanding, the longitudinal motion model of Boeing 747 is employed here [6].

$$\dot{x} = Ax + Bu \quad (1)$$

where the state vector $x = [u, w, q, \theta, h]^T$, the input vector $u = [\delta_e, \delta_t]^T$. u is the horizontal ground

speed, w is the vertical ground speed, q is the pitch rate, θ is the pitch angle, h is the altitude, δ_e is the elevator deflection, δ_t is the thrust force. The air speed of aircraft V and angle of attack α are commonly used which can be represented as follows:

$$V = \sqrt{u^2 + w^2} \quad (2)$$

$$\alpha = \tan^{-1}(w/u) \quad (3)$$

For $w^2 \ll u^2$ in the landing maneuver, the approximated relations are

$$V \cong u \quad (4)$$

$$\alpha \cong w/u \quad (5)$$

And the flight path angle $\gamma = \theta - \alpha$.

The A, B matrices are obtained according to aerodynamic derivatives of Boeing 747, which are given as follows [6]:

$$A = \begin{bmatrix} -0.0210 & 0.1220 & 0.0000 & -0.3220 & 0.0000 \\ -0.2090 & -0.5300 & 2.2100 & 0.0000 & 0.0000 \\ 0.0170 & -0.1640 & -0.4120 & 0.0000 & 0.0000 \\ 0.0000 & 0.0000 & 1.0000 & 0.0000 & 0.0000 \\ 0.0000 & -1.0000 & 0.0000 & 2.2100 & 0.0000 \end{bmatrix}, B = \begin{bmatrix} 0.0100 & 1.0000 \\ -0.0640 & -0.0440 \\ -0.3780 & 0.5440 \\ 0.0000 & 0.0000 \\ 0.0000 & 0.0000 \end{bmatrix} \quad (6)$$

Eq. (7) and Eq. (8) represent the elevator model and engine model [7], respectively.

$$\frac{\delta_e}{\delta_{ec}} = \frac{10}{s+10} \quad (7)$$

$$\frac{\delta_t}{\delta_{tc}} = \frac{0.25}{s+0.25} \quad (8)$$

where δ_{ec} and δ_{tc} are commands.

2.2 LPV Model with Elevator Failure

Assume that the elevator failure factor enters in the aircraft model linearly. The longitudinal motion LPV model of Boeing 747 can be written as:

$$\dot{x} = Ax + B\begin{bmatrix} \rho & 0 \\ 0 & 1 \end{bmatrix} u \quad (9)$$

Where ρ is the scheduling parameter representing the elevator failure and $0 \le \rho \le 1$.

2.3 Description of the Landing Maneuver

Typically, there are four segments in the landing maneuver [8] (see Fig. 1): alignment, glide slope, flare and taxiing. The glide slope and flare segment are mainly studied in this paper as they are the most challenging segments.

1) Alignment: In this segment, the aircraft will align itself to the runway and the altitude will be maintained about 500m from ground.

2) Glide slope: The aircraft will enter the glide slope mode when the approach path reaches the desired glide path. In this segment, the flight path angle should be kept at -3deg and the gliding velocity should be maintained at a constant value, which is selected as 67.4m/s in this paper.

3) Flare: When the altitude is around 15m, the aircraft enters the flare segment. The aircraft will

gradually approach toward the ground and vertical speed will be reduced to 0.3m/s at the touch down point.

4) Taxiing: The last segment of the landing maneuver begins when the aircraft touches the runway and reduces its velocity quickly.

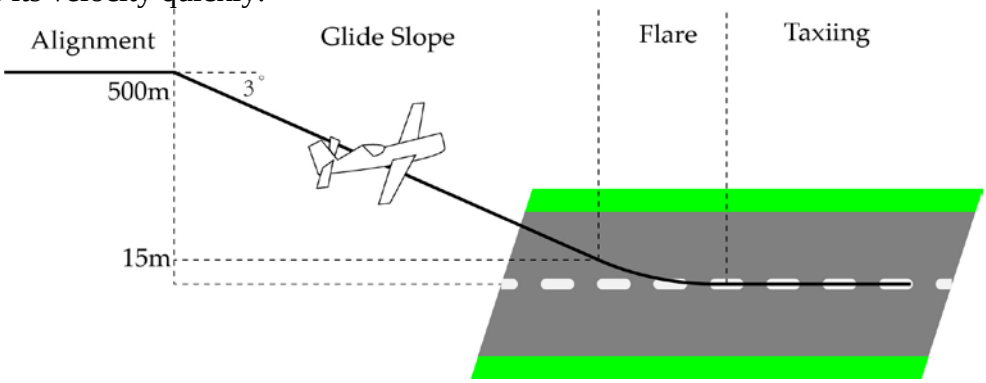

Fig. 1 Illustration of landing maneuver

3. FTC Autolanding System Design

The proposed FTC autolanding system is shown in Fig. 2, which includes a two-stage Kalman filter fault estimator, a civil aircraft system and an LPV controller. The fault parameter cannot be measured directly but can be estimated by the estimator module. The active fault-tolerant LPV controller is adaptive to the change of the estimated fault parameter. Note that the civil aircraft system is a function of the scheduling parameter.

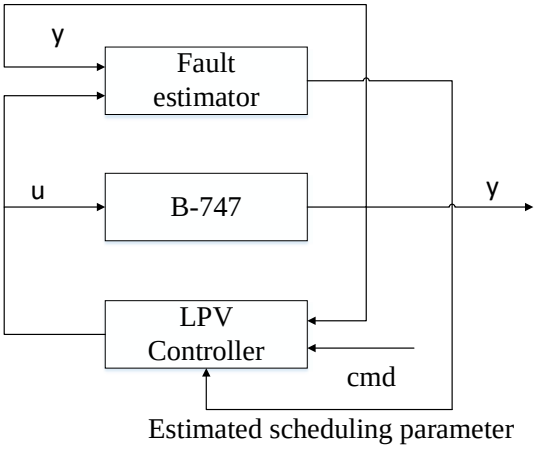

Fig. 2 FTC autolanding system structure

3.1 Robust LPV Control Synthesis

Consider an LPV system

$$\begin{bmatrix} \dot{x} \\ e \end{bmatrix} = \begin{bmatrix} A(\rho) & B(\rho) \\ C(\rho) & D(\rho) \end{bmatrix} \begin{bmatrix} x \\ d \end{bmatrix} \quad (10)$$

where ρ is the scheduling parameter. The LPV control design problem is to find a controller $K(\rho)$ such that the close-loop system is internally stable and the L_2 norm of d to e which is represented by γ is minimized. The controller $K(\rho)$ explicitly depends on the scheduling parameter. The main synthesis problem can be written as the following optimization:

$$\min_{X(\rho),Y(\rho)} \gamma \quad (11)$$

Subject to a set of linear matrix inequalities (LMIs) [9]. The controller $K(\rho)$ can be found from the solutions $X(\rho)$ and $Y(\rho)$ of the LMIs optimization problem.

Fig. 3 shows the interconnection structure for the LPV autolanding control design. In order to normalize the reference inputs, the altitude h_d and speed V_d commands are scaled by W_{in}. Select the average altitude $h_{ave} = 250m$ and average speed $V_{ave} = 67.4m/s$, and yields:

$$W_{in} = diag(h_{ave}, V_{ave}) = diag(250, 67.4) \quad (12)$$

As the altitude error e_h and the speed error e_V should be small, and the altitude and speed do not change quickly, the gain of W_{out} should be big enough at low frequency to enable the control system to track ramp commands with a very small steady state error. Hence, the W_{out} is selected as:

$$W_{out} = diag\left(20000\frac{1}{s+0.007}, 12000\frac{1}{s+0.002}\right) \quad (13)$$

As the maximum pitch rate is ± 3 deg/s [7], the weight function of W_p is selected as:

$$W_p = \frac{57.3}{3} \quad (14)$$

The weight function of W_{act} is applied to confine the control deflections and their rates. According to the maximum deflections and rates of elevator and engine [7], the W_{act} is selected as:

$$W_{act} = diag\left(\frac{57.3}{20}, \frac{57.3}{15}, \frac{57.3}{5}, \frac{57.3}{1}\right) \quad (15)$$

As measurements are often corrupted with some noises, according to the measurement noise error [7], the measurement noise weight function W_n is selected as:

$$W_n = diag\left(W_{nh}, W_{\dot{n}h}, W_{nV}, W_{\dot{n}V}, W_{nq}, W_{n\theta}\right) = diag\left(0.01, 0.025, 0.015, 0.02, \frac{0.05}{57.3}, \frac{0.1}{57.3}\right) \quad (16)$$

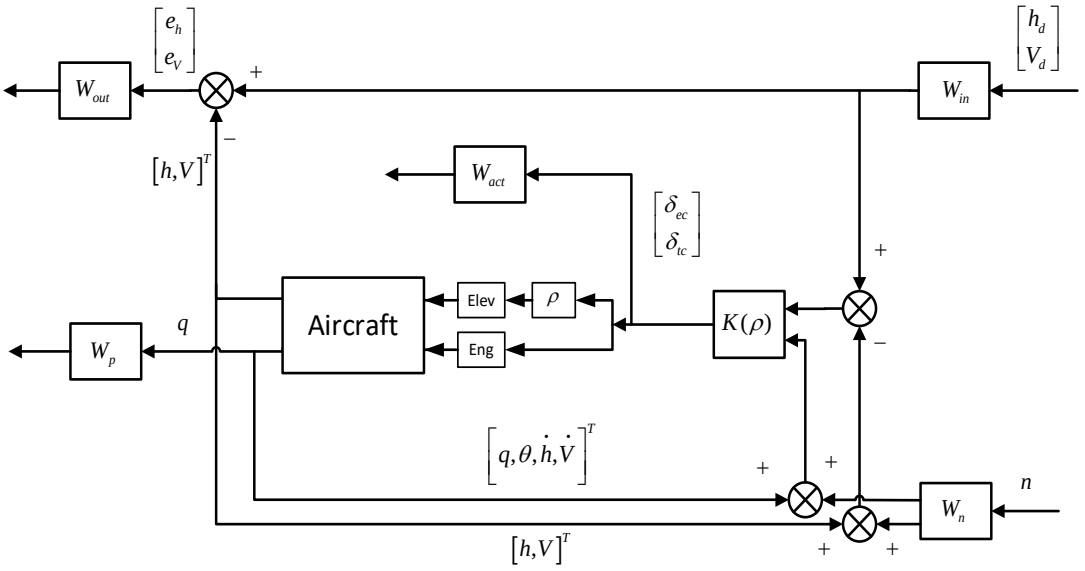

Fig. 3 Interconnection structure for LPV autolanding control

3.2 Two-Stage Kalman Filter Estimator

The estimator is based on a linear discrete model, which is formed as [10]:

$$
\begin{aligned}
x_{k+1} &= A_k^d x_k + B_k^d u_k + \begin{bmatrix} b_1^d \gamma_k^1 & b_2^d \gamma_k^2 & \cdots & b_l^d \gamma_k^l \end{bmatrix} \begin{bmatrix} u_k^1 \\ u_k^2 \\ \vdots \\ u_k^l \end{bmatrix} + w_k^x \\
&= A_k^d x_k + B_k^d u_k + E_k^d \gamma_k + w_k^x \\
\gamma_{k+1} &= \gamma_k + w_k^\gamma \\
y_{k+1} &= C_{k+1}^d x_{k+1} + v_{k+1}
\end{aligned} \tag{17}
$$

where $x_k \in R^{n_x}$, $u_k \in R^{n_u}$, $\gamma_k \in R^{n_u}$, and $y_k \in R^{n_y}$ are the state, input, bias and output variables, respectively. The noise sequences w_k^x, w_k^γ, and v_k denote the uncorrelated white Gaussian noise sequences with zero means.

$$
E = \left\{ \begin{bmatrix} w_k^x \\ w_k^\gamma \\ v_k \end{bmatrix} \begin{bmatrix} w_j^x & w_j^\gamma & v_j \end{bmatrix} \right\} = \begin{bmatrix} Q_k^x & 0 & 0 \\ 0 & Q_k^\gamma & 0 \\ 0 & 0 & R_k \end{bmatrix} \delta_{kj} \tag{18}
$$

where $Q_k^x > 0$, $Q_k^\gamma > 0$, $R_k > 0$, and δ_{kj} is the Kronecker delta. The bias vector γ with element $-1 \le \gamma_k^i \le 0$ relates an actuator failure parameter.

The algorithm of the two-stage Kalman filter is given as follows [11]:

1) Optimal bias estimator

$$
\begin{aligned}
\hat{\gamma}_{k+1|k} &= \hat{\gamma}_{k|k} \\
P_{k+1|k}^\gamma &= P_{k|k}^\gamma + Q_k^\gamma \\
\hat{\gamma}_{k+1|k+1} &= \hat{\gamma}_{k+1|k} + K_{k+1}^\gamma (\bar{r}_{k+1} - H_{k+1|k} \hat{\gamma}_{k|k}) \\
K_{k+1}^\gamma &= P_{k+1|k}^\gamma H_{k+1|k}^T (H_{k+1|k} P_{k+1|k}^\gamma H_{k+1|k}^T + \bar{S}_{k+1})^{-1} \\
P_{k+1|k+1}^\gamma &= (I - K_{k+1}^\gamma H_{k+1|k}) P_{k+1|k}^\gamma
\end{aligned} \tag{19}
$$

where the filter residual $\bar{r}_{k+1} = y_{k+1} - C_{k+1}^d \bar{x}_{k+1|k}$.

2) Bias-free state estimator

$$
\begin{aligned}
\bar{x}_{k+1|k} &= A_k^d \bar{x}_{k|k} + B_k^d u_k + W_k \hat{\gamma}_{k|k} - V_{k+1|k} \hat{\gamma}_{k|k} \\
\bar{P}_{k+1|k}^x &= A_k^d \bar{P}_{k|k}^x \left(A_k^d \right)^T + Q_k^x + W_k P_{k|k}^\gamma W_x^T - V_{k+1|k} P_{k+1|k}^\gamma V_{k+1|k}^T \\
\bar{x}_{k+1|k+1} &= \bar{x}_{k+1|k} + \bar{K}_{k+1}^x (y_{k+1} - C_{k+1}^d \bar{x}_{k+1|k}) \\
\bar{K}_{k+1}^x &= \bar{P}_{k+1|k}^x \left(C_{k+1}^d \right)^T \left\{ C_{k+1}^d \bar{P}_{k+1|k}^x \left(C_{k+1}^d \right)^T + R_{k+1} \right\}^{-1} \\
\bar{P}_{k+1|k+1}^x &= (I - \bar{K}_{k+1}^x C_{k+1}^d) \bar{P}_{k+1|k}^x
\end{aligned} \tag{20}
$$

where the filter residual covariance $\bar{S}_{k+1} = C_{k+1}^d \bar{P}_{k+1|k}^x \left(C_{k+1}^d \right)^T + R_{k+1}$.

3) Coupling equations

$$
\begin{aligned}
W_k &= A_k^d V_{k|k} + E_k^d \\
V_{k+1|k} &= W_k P_{k|k}^{\gamma} \left(P_{k+1|k}^{\gamma} \right)^{-1} \\
H_{k+1|k} &= C_{k+1}^d V_{k+1|k} \\
V_{k+1|k+1} &= V_{k+1|k} - \overline{K}_{k+1}^{x} H_{k+1|k}
\end{aligned} \tag{21}
$$

4) Compensated state and error covariance estimator

$$
\begin{aligned}
\hat{x}_{k+1|k+1} &= \bar{x}_{k+1|k+1} + V_{k+1|k+1} \hat{\gamma}_{k+1|k+1} \\
P_{k+1|k+1} &= \overline{P}_{k+1|k+1}^{x} + V_{k+1|k+1} P_{k+1|k+1}^{\gamma} + V_{k+1|k+1}^{T}
\end{aligned} \tag{22}
$$

After estimating the $\hat{\gamma}$, the estimated scheduling fault parameter $\hat{\rho}$ can be written as:

$$
\hat{\rho} = 1 + \hat{\gamma} \tag{23}
$$

4. Simulation and Analysis

In this section, the proposed LPV autolanding controller is applied to control the civil aircraft landing maneuver for pre-defined elevator failure. The scheduling fault parameter is

$$
\rho = \begin{cases} 1 & 0 \le t \le 50s \\ 0.7 & 50s < t \le 100s \\ 0.2 & t > 100s \end{cases} \tag{24}
$$

The covariance matrices Q_k^x, Q_k^{γ}, R_k are given as follows:

$$
\begin{aligned}
Q_k^x &= 3diag(1, 0.01^2, 0.01^2, 0.01^2, 0.01^2) \\
Q_k^{\gamma} &= 3diag(0.05^2, 0.05^2) \\
R_k &= 3diag(0.01^2, 0.01^2)
\end{aligned} \tag{25}
$$

The initial values of covariance matrices $P_{0|0}^{\gamma}$ and $\overline{P}_{0|0}^{x}$ are set as:

$$
\begin{aligned}
P_{0|0}^{\gamma} &= 10 I_2 \\
\overline{P}_{0|0}^{x} &= 10 I_5
\end{aligned} \tag{26}
$$

For the purpose of comparison, an H_{∞} controller is designed at $\rho = 1$ (without failure) with the same weight functions described in section 3.1. The simulation results of the LPV and H_{∞} controller are shown in Fig. 4.

The altitude responses and altitude errors are shown in Fig. 4(a) and Fig. 4(b), respectively. It is obvious that when the elevator failure occurs after 50s, the altitude error of the H_{∞} controller changes 2m up and down, when a severe failure occurs after 100s, it changes about 10m, while the LPV controller almost has no change. It is also expected that the vertical speed is slow and smooth. As seen from Fig. 4(c), the vertical speed of the H_{∞} controller changes 0.5m/s and 1m/s at the two failure occurrences compared with the LPV controller. The air speed of the LPV controller is more closed to the desired speed 67.4m/s while the H_{∞} controller has a 1m/s-3m/s variation, see Fig. 4(d). Fig. 4(e) shows the responses of pitch angle and Fig. 4(f) shows the responses of pitch rate. It can be seen that the pitch angle and the pitch rate of the LPV controller are smoother. But at the transition

from glide slope to flare, the variations of the LPV controller are more intense which means the LPV controller tracks the trajectory more quickly and closely.

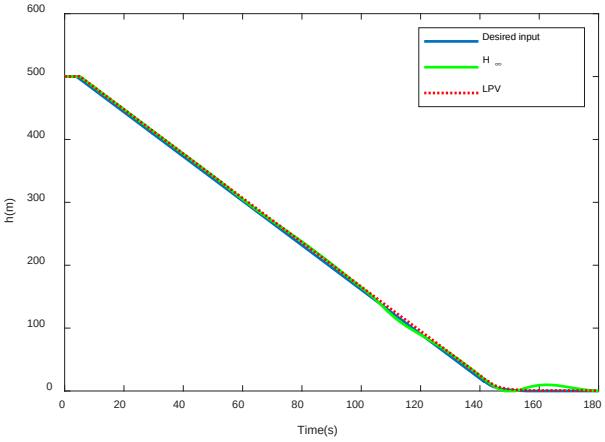

(a) Altitude responses

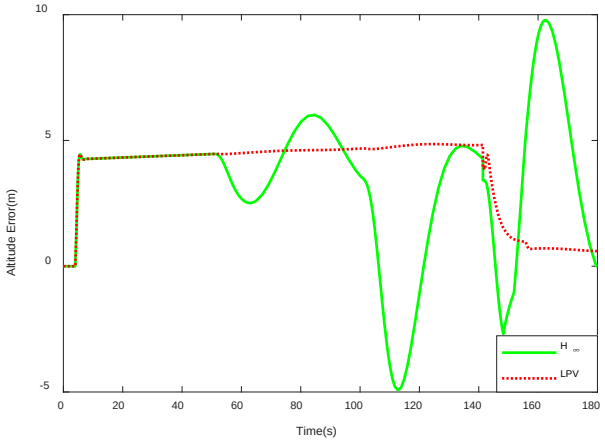

(b) Altitude errors

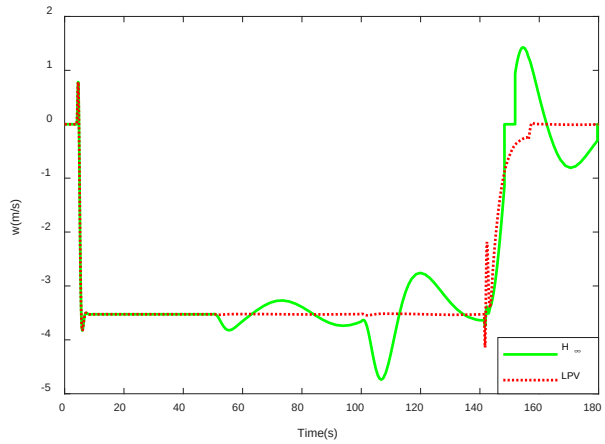

(c) Vertical speed responses

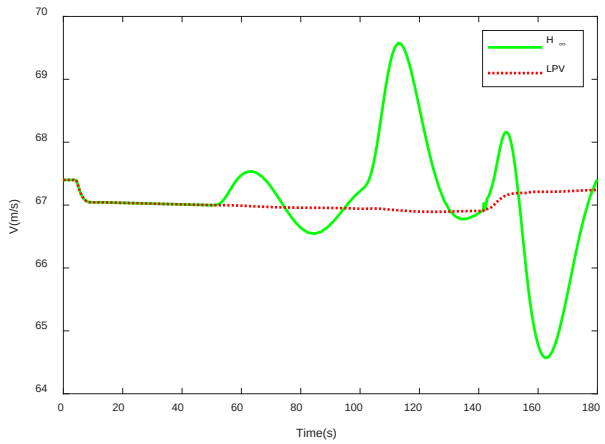

(d) Air speed responses

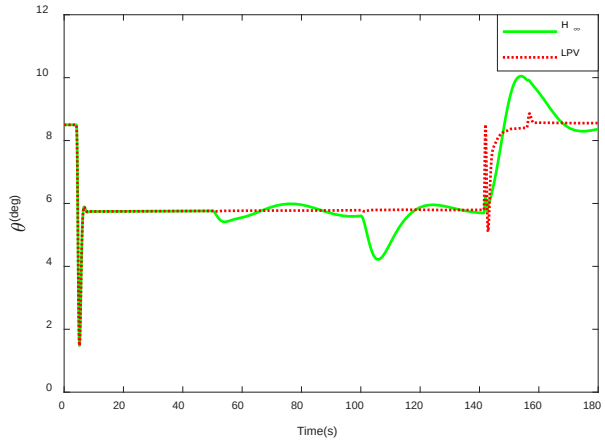

(e) Pitch angle responses

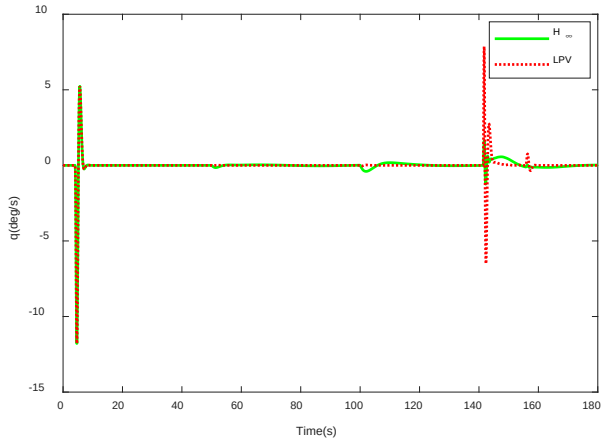

(f) Pitch rate responses

Fig. 4 Time responses of aircraft with LPV and H_∞ controllers

5. Conclusions

This paper presented a new approach to the FTC autolanding system of the civil aircraft. Differently from the existing control methods for the autolanding system, this approach exploited the integration of the LPV controller and two-stage Kalman filter, which was an active FTC scheme for elevator failure. According to the desired performances, the weight functions of LPV controller were

selected. The algorithm of the two-stage Kalman filter was given to estimate the failure parameter. The simulation results demonstrated the fault-tolerant capacity of the proposed scheme.

Acknowledgments

This work was financially supported by the National Natural Science Foundation of China, grant number 10577012, and the Chinese Aviation Science Fund, grant number 20160757001.

References

[1] J.M. Bai, H.J. Rong. 2012. Fault-tolerant autolanding controller design using neural network. Chinese Control Conference, July 25-27, Hefei, China.

[2] A.A. Pashilkar, N. Sundararajan, P. Saratchandran. 2006. A fault-tolerant neural aided controller for aircraft auto-landing. *Aerospace Science and Technology*, Vol. 10(49-61).

[3] J. Lee, H.S. Choi, S. Lee, et al. 2012. Time Delay Fault Tolerant Controller for Actuator Failures during Aircraft Autolanding. *Transactions of the Japan society for Aeronautical and space sciences*, Vol. 55(175-182).

[4] Z. Liu, Y. Zhang, C. Yuan, et al. 2015. An Adaptive Linear Parameter Varying Fault Tolerant Control Scheme for Unmanned Surface Vehicle Steering Control. Chinese Control Conference, July 28-30, Hangzhou, China.

[5] Z. Liu, C. Yuan, Y. Zhang. 2017. Active Fault-Tolerant Control of Unmanned Quadrotor Helicopter Using Linear Parameter Varying Technique. *Journal of Intelligent & Robotic Systems*, Vol. 88(415-436).

[6] A.E. Bryson. 1994. Control of Spacecraft and Aircraft. *Princeton University Press, Princeton, NJ*.

[7] B.W. Parkinson, M.L. O'Connor, K.T. Fitzgibbon. 1996. Aircraft Automatic Approach and Landing Using GPS. *Global Positioning System: Theory and Applications*, Vol. 2(397-425).

[8] P. Serra, R. Cunha, T. Hamel, C. Silvestre, F. Le Bras. 2015. Nonlinear image-based visual servo controller for the flare maneuver of fixed-wing aircraft using optical flow. *IEEE Transactions on Control Systems Technology*, Vol. 23(570–583**)**.

[9] J.Y. Shin. 2000. Wost-Case Analysis and Linear Parameter-Varying Gain-Scheduled Control of Aerospace Systems. Ph.D. thesis, *Department of Aerospace Engineering and Mechanics, University of Minnesota*.

[10] J.Y. Shin, N.E. Wu, C. Belcastro. 2004. Adaptive Linear Parameter Varying Control Synthesis for Actuator Failure. *Journal of Guidance, Control, and Dynamics*, Vol. 27(787-794).

[11] N.E. Wu, Y. Zhang, K. Zhou. 2000. Detection, Estimation, and Accommodation of Loss of Control Effectiveness. *International Journal of Adaptive Control and Signal*, Vol. 14(775–795).